Published in final edited form as:
J Comp Neurol. 2009 June 10; 514(5): 449–458. doi:10.1002/cne.22016.

Regulation of Neonatal Development of Retinal Ganglion Cell Dendrites by Neurotrophin-3 Overexpression

Xiaorong Liu[1,2,3,*], **Michael L. Robinson**[6], **Ann Marie Schreiber**[2], **Vincent Wu**[2], **Matthew M. LaVail**[2,4,5], **Jianhua Cang**[1], and **David R. Copenhagen**[2,3,5,*]

[1] Department of Neurobiology and Physiology, Northwestern University, Evanston, IL 60208

[2] Department of Ophthalmology, University of California, San Francisco, San Francisco, California 94143

[3] Department of Physiology, University of California, San Francisco, San Francisco, California 94143

[4] Department of Anatomy, University of California, San Francisco, San Francisco, California 94143

[5] Program in Neuroscience, University of California, San Francisco, San Francisco, California 94143

[6] Department of Zoology, Miami University, Oxford, OH 45056

Abstract

The morphology of dendrites constrains and reflects the nature of synaptic inputs to neurons. The visual system has served as a useful model to show how visual function is determined by the arborization patterns of neuronal processes. In retina, light ON and light OFF responding ganglion cells selectively elaborate their dendritic arbors in distinct sublamina, where they receive, respectively, inputs from ON and OFF bipolar cells. During neonatal maturation, the bi-laminarly distributed dendritic arbors of ON-OFF RGCs are refined to more narrowly localized monolaminar structures characteristic of ON or OFF RGCs. Recently, brain-derived neurotrophic factor (BDNF) has been shown to regulate this laminar refinement, and, additionally, to enhance the development of dendritic branches selectively of ON RGCs. Although other related neurotrophins are known to regulate neuronal process formation in the central nervous system, little is known about their action in maturing retina. Here, we report that overexpression of neurotrophin-3 (NT-3) in the eye accelerates RGC laminar refinement before eye opening. Furthermore, NT-3 overexpression increases dendritic branch number but reduces dendritic elongation preferentially in ON-OFF RGCs, a process that also occurs before eye opening. NT-3 overexpression does affect dendritic maturation in ON RGCs, but to a much less degree. Taken together, our results suggest that NT-3 and BDNF exhibit overlapping effects in laminar refinement but distinct RGC-cell-type specific effects in shaping dendritic arborization during postnatal development.

Keywords

Neurotrophin-3 (NT-3); Retinal Ganglion Cells; Dendritic Development; Brain-Derived Neurotrophic Factor (BDNF); Transgenic Mice; Confocal Imaging

[*]Corresponding authors: Xiaorong Liu, Ph.D., Tel: 847-467-0529; Fax: 847-491-5211; xiaorong-liu@northwestern.edu; and David Copenhagen, Ph.D., Tel: 415-476-2527; Fax: 415-476-6289; cope@phy.ucsf.edu.

Introduction

Retinal ganglion cells (RGCs) encode and convey visual signals from the eye to higher centers in the brain. Functional properties of RGCs' responses to visual stimulation are governed by their characteristic dendritic morphology (Sernagor *et al.*, 2001). We, and others, demonstrated that after eye opening, ON-OFF RGCs, which have bi-laminated dendrites and respond to both light onset and offset, are gradually converted into mono-laminated ON and OFF RGCs, and this process requires visual experience (Tian and Copenhagen, 2003; Landi *et al.*, 2007; Liu *et al.*, 2007). Furthermore, following eye opening, the dendrites of ON RGCs, but not ON-OFF RGCs, elongate by the addition of branches (Liu *et al.*, 2007). Visual deprivation suppresses the formation of new branches in these ON RGCs (Liu *et al.*, 2007). Using transgenic and mutant mice to perturb neurotrophin signaling *in vivo*, we discovered that vision-induced refinement of RGC dendrites is modulated by brain-derived neurotrophic factor (BDNF) signaling (Liu *et al.*, 2007). Compared to the recent progress in the study of RGC development after eye opening, the temporal and spatial changes of RGC dendritic morphologies *before* eye opening and their regulation by neurotrophins have not been characterized.

Neurotrophin-3 (NT-3) has been implicated in modulating both the axonal and dendritic morphology of neurons in the central nervous system (CNS; McAllister *et al.*, 1999). For example, NT-3 causes fibers to be more densely packed by increasing the fasciculation and branching in cultured cerebellar granule cells (Segal *et al.*, 1995). In slice cultures of cortical neurons, NT-3 stimulated dendritic growth in layer 6 and inhibited BDNF-stimulated dendritic growth in layer 4 (McAllister *et al.*, 1997). NT-3 is expressed in vertebrate retina (Hallbook *et al.*, 1996; Bennett *et al.*, 1999; Seki *et al.*, 2004). In mouse retina, BDNF and NT-3 are expressed both pre- and postnatally (Bennett *et al.*, 1999). BDNF levels gradually increase with age after birth (Liu *et al.*, 2007), while how NT-3 levels change during postnatal maturation of the retina remains unknown. Visual experience controls BDNF levels in rat and mouse (Seki *et al.*, 2003; Liu *et al.*, 2007), but not NT-3 levels (Seki *et al.*, 2004). Given the different actions of BDNF and NT-3 in the CNS and the dissimilar regulation of their expression by activity, we explored the hypothesis that they may play different roles in RGC dendritic development.

In this study, we use a well characterized *in vivo* model system (Tian and Copenhagen, 2003; Landi *et al.*, 2007; Liu *et al.*, 2007) to study the developmental profile of RGC dendritic structures before eye opening. We confirm that the RGC laminar refinement commences well before the time of eye opening, consistent with other studies (Tian and Copenhagen, 2003; Coombs *et al.*, 2007; Landi *et al.*, 2007). More importantly, different types of RGCs exhibit different temporal patterns in their dendritic growth. In mice overexpressing NT-3 in the eye (NT-3 OE), we find that dendritic areas subtended by ON-OFF RGCs are smaller than in age-matched wild type (WT) mice at P13. Furthermore, compared to BDNF overexpression that facilitates the developmental formation of new branches in ON but not ON-OFF RGCs, NT-3 overexpression increases dendritic branching and inhibits dendritic elongation preferentially in ON-OFF RGCs. Taken together, our results suggest that overexpression of NT-3 and BDNF exert overlapping and distinct actions in RGC laminar refinement and in the sculpting of dendritic arbors during postnatal development.

Materials and Methods

Animals

Transgenic mice expressing NT-3 driven alpha A-crystallin promoter from the lens were generated (lines OVE 613 and 614, Robinson *et al.*, 1995). In brief, a rat NT-3 clone was

inserted into the crystallin promoter vector CPV2, which contains the −288/+43 alpha A-crystallin promoter at the 5′ end and SV40 intron and polyadenylation sequences at the 3′ end (Robinson *et al.*, 1995). The injections and screening of transgenic mice are fully described in Lavail *et al.*, 2008. Thy-1-YFP transgenic mice with C57BL/6 background (Feng *et al.*, 2000; Liu *et al.*, 2007) were crossed with NT-3 transgenic mice (labeled as NT-3 OE in this paper) to examine dendritic structures of RGCs. NT-3 OE on the BALB/c genetic background were crossed five to ten times with C57BL/6, so NT-3 OE mice were mainly on C57BL/6 background.

Transgenic mice were identified by PCR using genomic DNA isolated from clipped tails (Liu *et al.*, 2007). Thy-1-YFP was identified according to (Feng *et al.*, 2000; Liu *et al.*, 2007). PCR primers used to identify NT-3 OE mice were SV40A (5′-GTGAAGGAACCTTACTTCTGTGGTG-3′) and SV40B (5′-GTCCTTGGGGTCTTCTACCTTTCTC-3′), which span the intron in the SV40-derived sequences (Lavail *et al.*, 2008). Mice were reared in 12h light/12h darkness from birth or constant darkness from Postnatal (P) day 2–3. Transgenic lines OVE 613 and 614 exhibited similar phenotypes (data not shown) and results shown in this paper were from OVE 613. All animal procedures conformed to the guidelines on the Use of Animals in Neuroscience Research from the NIH and were in accordance with protocols approved by the University of California, San Francisco and Northwestern University.

Analysis of NT-3 Expression in the Mouse Retina

Retinal proteins were isolated and Western blots and immunohistochemistry were performed (Johnson *et al.*, 2004; Liu *et al.*, 2007). The primary antibodies used in this study and their sources are listed in Table 1. For our purposes we confirmed the expected specificity of the antibodies by omitting the primary antibodies or substituting normal rabbit or goat serum for polyclonal antibodies. More rigorous characterization of each of the antibodies we used is described below Table 1.

Anti-Brn-3a clone 5A3.2 antibody (Chemicon) was generated against POU-domain (Amino acids 186–224 of Brn-3a fused to the T7 gene 10 protein; Xiang *et al.*, 1995). It labels only ganglion cells in a variety of vertebrate retinas, including mouse retina (Gerrero *et al.*, 1993; Xiang *et al.*, 1995). The antibody showed no reactivity in Brn-3a knock-out mice (Xiang *et al.*, 1996).

Monoclonal anti-calbindin-D-28K antibody was generated against bovine kidney calbindin-D (Sigma). It was found to label horizontal cells and amacrine cells in the mouse retina (Haverkamp and Wassle, 2000). This labeling was abolished in a calbindin knockout mouse (Wassle *et al.*, 1998; Haverkamp and Wassle, 2000).

GFP-Alexa Fluor® 488 conjugate was made from the rabbit anti-GFP IgG fraction (Invitrogen, CA). The anti-GFP rabbit polyclonal antibody was raised against GFP isolated directly from *Aequorea victoria* and the IgG fraction is purified by ion-exchange chromatography, according to the manufacturer data sheet (Invitrogen, CA). It is widely used for detection of GFP signals by Western blot analysis and immunohistochemistry (Tian and Copenhagen, 2003; Liu *et al.*, 2007). No immunoreactivity was observed with this antibody in native mouse retina (data not shown).

Anti-human NT-3 antibody was produced in goats immunized with purified, insect cell line Sf 21-derived, recombinant human Neurotrophin-3 (rhNT-3). The specificity of this antibody has been fully characterized by ELISA and immunostaining in the mouse retina (Lavail *et al.*, 2008). In NT-3 overexpressing mice NT-3 labeling is increased *(*Lavail *et al.*,

2008). In Western blots, NT-3 antibody visualizes a 27 kDa homodimer band of two 13.6 kDa monomers (see Fig. 1A).

Mouse monoclonal anti-TH was raised against purified TH from PC12 cells (Chemicon, now Millipore). In Western blots, it recognizes a protein of approximately 59–63 kDa, which corresponds to that estimated for TH (Chemicon data sheet). In mouse retina, this TH antibody only stains one class of amacrine neuron showing intrinsic dopamine fluorescence (Witkovsky *et al.*, 2008).

Rabbit anti-CaBP5 polyclonal antibody was raised against bacterially expressed CaBP5 in New Zealand White rabbits (Haeseleer *et al.*, 2000; Cocalico Biologicals, Inc., Reamstown, PA). Partial sequences of CaBP5 were confirmed as predicted from the 18-and 16-kDa bands recognized by CaBP5 antibody on SDS-PAGE with the bovine retina extract (Haeseleer *et al.*, 2000). In the mouse retina, expression of CaBP5 is restricted to retinal rod and cone bipolar cells (Haeseleer *et al.*, 2000; Liu *et al.*, 2007).

SMI-32 is a monoclonal antibody against the nonphosphorylated neurofilament H in homogenized hypothalami from Fischer 344 rat brain (Sternberger Monoclonal Inc. is now part of Covance, Princeton, NJ). Two bands of appropriate molecular weight (200 and 168 kDa) were seen in Western blots with monkey and human neocortex extracts (Campbell and Morrison, 1989). It was originally reported to selectively mark alpha-type RGCs in the mouse retina (Nixon *et al.*, 1989). More studies showed that it actually stains 4 classes of RGC--M3, M7, M9 and M10 (Nixon *et al.*, 1989; Coombs *et al.*, 2006; Liu *et al.*, 2007).

For immunostaining, retinas were dissected and fixed in 4% (w/v) paraformaldehyde (PFA) in 0.1 M phosphate-buffered saline (PBS, pH 7.4) at P9–11 (labeled as P10 for simplification), P12–13 (labeled as P13), P27–32 (labeled as P28), P47–52 (labeled as P50), and P180 (Liu *et al.*, 2007). For sections, eyes were stored overnight in 25% sucrose in 0.1 M PBS at 4°C and embedded in optimum cutting temperature (OCT) compound (Tissue-Tek, Elkhart, IN). Sections of the retina were cut perpendicular to the vitreal surface with a cryostat at 12–16 μm. Cryostat sections or whole-mounted retinas were washed in 0.1 M PBS, incubated for 1 or 2 nights in primary antibody with 0.5 or 1% Triton X-100 and 10% normal goat serum at 4°C, and then washed in 0.1 M PBS. To visualize binding of the primary antibodies, sections or whole-mounted retinas were incubated in secondary antibody conjugated to Alexa Fluor 488, or Alexa Fluor 594 (diluted 1:500–1:1,000; Molecular Probes, Eugene, OR) for 1–2 hours at room temperature or overnight at 4°C, and then cover slipped with Vectashield mounting medium (Vector, Burlingame, CA). For confocal microscopy, images were captured with a Zeiss Pascal confocal microscope (Zeiss, Thornwood, NY; Johnson *et al.*, 2004; Liu *et al.*, 2007).

Two methods were used to measure the inner plexiform layer (IPL) thickness: a) In fixed retinas, cut radially at ~13 μm thick sections, the IPL thickness was measured at 5–10 points across the extent of the retina; b) In whole-mounted retina, the IPL thickness = (the average of the number of confocal sections -1) × (the interval between sections). We compared the IPL thickness measured by above two methods in the same age group of animals and found no difference (data not shown).

For Western blotting, mouse retinas were harvested and cytoplasmic and nuclear proteins were prepared using the NE-PER extraction reagents (Pierce Biotechnology, Rockford, IL). The protein concentrations were determined with a BCA Protein Assay Kit (Pierce Biotechnology). 15–20 μg of extract were resolved on Novex-NuPAGE 4–12% BT gels (Invitrogen) and transferred to PVDF membranes (Invitrogen). After blocking with 5% nonfat milk in washing buffer (1× PBS + 0.1% Tween-20) at room temperature for 1 hour, the membranes were incubated with NT-3 antibody at 4°C overnight. After washing, the

blots were incubated with goat antiperoxidase-conjugated secondary antibodies (1:4,000; Amersham Biosciences, Piscataway, NJ) at room temperature for 2–3 hours. Finally, the proteins on the membranes were detected by using the ECL+ chemiluminescence system (Amersham Biosciences). The blots were incubated with stripping buffer (100 nM 2-mercaptoethanol, 2% sodium dodecyl sulfate, and 62.5 mM Tris-HCl, pH = 6.7) at 50°C for 0.5–1 hour. The blots were then re-probed with mouse glyceraldehyde-phosphate dehydrogenase (GAPDH) antibody (Chemicon International; 1:500) as an internal control. No bands were detected when the primary antibody was omitted (data not shown).

Detection and Analyses of RGC Dendritic Structure

Z-stack images of YFP-expressing RGCs were collected using a Zeiss confocal laser-scanning microscope (Tian and Copenhagen, 2003; Liu *et al.*, 2007). The identification and classification of RGCs and their dendritic tracing are described in Liu *et al.* (2007). In brief, optical sections obtained with a Zeiss Pascal confocal microscope were collected at intervals of 0.8 –1.5 μm for each RGC. If the terminal dendrites of a RGC were seen exclusively in the top two-fifths of the total sections, it was classified as an OFF RGC; if the terminal dendrites of an RGC were seen in the bottom three-fifths of the total sections, it was classified as an ON RGC; RGCs that had processes in sublamina *a* or *b* and showed processes in more than one optical section across the sublamina *a*/*b* border were classified as ON-OFF RGCs (Liu *et al.*, 2007). This is a functional definition that implicitly assumes synaptic processes in either sublamina *a* or *b* will be driven synaptically by axonal terminals from either OFF or ON bipolar cells.

To determine dendritic coverage of RGC arbors, z-stack images of YFP-expressing RGCs were projected to a single 2D-plane and coverage area was measured by drawing a convex polygon linking the outermost dendritic tips (Diao *et al.*, 2004; Liu *et al.*, 2007). The RGC dendritic length and the number of branches were measured using NIH ImageJ (Liu *et al.*, 2007). One-way ANOVA-tests were performed using GraphPad Prism to compare multiple samples in one group, and Student's *t*-tests were performed to compare paired samples. All data sets were examined by a second observer to cross-check classification and tracing of RGCs. Adobe Photoshop CS (Adobe Systems, San Jose, CA) was used to adjust the contrast, brightness, and sharpness for the preparation of photomicrographic figures.

Results

Expression of NT-3 in WT and NT-3 OE Retina

We confirmed previous findings in WT mice that NT-3 is expressed in the inner retina, especially in the RGCs (Fig. 1; Rickman and Brecha, 1995;Bennett *et al.*, 1999;Seki *et al.*, 2004). Western blots reveal that retinal NT-3 expression remains constant during mouse postnatal development (Fig. 1A), consistent with previous findings in the rat retina (Seki *et al.*, 2004). We further found that, in contrast to BDNF (Liu *et al.*, 2007), NT-3 expression was not affected by visual experience (Fig. 1B). Dark rearing (DR) did not change the expression level of NT-3 protein in the retina, compared to age matched controls raised in 12 hr dark/12 hr light cycles (Normal Rearing, NR; $P = 0.69$, Student's *t*-test, Fig. 1B). Immunohistochemical analysis showed that NT-3 co-localized with Brn3a, an RGC marker (Fig. 1C). NT-3 was also found in horizontal cells and subpopulations of amacrine cells, as revealed by calbindin and tyrosine hydroxylase (TH) staining (Fig. 1E, F). NT-3 was not found in bipolar cells labeled by calcium-binding protein 5 (CaBP5, Fig. 1D).

To study whether NT-3 modulates RGC dendritic development, we used transgenic mice that continuously overexpress NT-3 from lens fibers under the control of the αA-crystallin promoter (Lavail *et al.*, 2008). Retinal NT-3 protein levels were elevated more than 2-fold in

NT-3 OE mice (Lavail *et al.*, 2008). Consistent with increased retinal expression assessed by ELISA (Lavail *et al.*, 2008), immunostaining with NT-3 antibody showed that the overall level of NT-3 detected in the inner retina was higher in NT-3 OE mice (Fig. 1G). Lavail *et al.* (2008) showed NT-3 OE mice on a BALB/c background exhibited normal retinal morphology as assessed by light microscopy in plastic embedded sections. We examined retinas of NT-3 OE mice on a C57BL/6 background and found normal appearing retinas (data not shown). We also immunostained NT-3 OE retinas with anti-CaBP5 and found no discernible difference between NT-3 OE and WT mice (Fig. 1H). We quantified the IPL thickness in NT-3 OE and WT mice and found no difference at either P13 (N = 6, $P = 0.07$) or at P28 (N = 6, $P = 0.49$ in Student's *t*-tests, Fig. 1I). Below we compare the rates of laminar refinement in WT to NT-3 OE mice during neonatal development.

Laminar Refinement of RGC Dendrites Begins Before Eye Opening

The percentage of bi-laminar (ON-OFF) RGCs is reduced at P28 compared to P13, the approximate age of eye opening (Tian and Copenhagen, 2003; Liu *et al.*, 2007). The reduction of the percentage of ON-OFF RGCs is taken as evidence of continuing laminar refinement after eye opening. Here, we characterized the developmental profile of RGC dendritic laminar structure before eye opening (Fig. 2A–B). We quantified the arborization patterns of RGC dendrites from Z-stacked confocal images taken of RGCs expressing yellow fluorescence protein (YFP) in Thy-1-YFP transgenic mice (Feng *et al.*, 2000; Tian and Copenhagen, 2003; Liu *et al.*, 2007). RGCs were classified into mono-laminated ON or OFF cells and bi-laminated ON-OFF cells based on their dendritic ramification level within the IPL, measured as the z-axis reading from the confocal microscope (Tian and Copenhagen, 2003; Badea and Nathans, 2004; Landi *et al.*, 2007; Liu *et al.*, 2007). Our previous results showed that approximately 28 % fewer ON-OFF RGCs are found in P28 mice compared to P13 mice (Liu *et al.*, 2007). Here we extended these findings to earlier ages and discovered that around 18 % fewer ON-OFF RGCs are found at P13 compared to P10, indicating that laminar refinement reflected by the loss of ON-OFF RGCs and subsequent increase in ON and OFF RGCs commences well before eye opening. At P10, 65.9 ± 1.4% of RGCs were bi-laminated ON-OFF type; at P13, around the time of eye opening, the percentage decreased to 54.1 ± 2.2%; and two weeks after eye opening at P28, it dropped to 39.2 ± 2.4% ($P < 0.001$ in one-way ANOVA, Fig. 2A). Over the same period, ON RGCs increased from 27.1 ± 4.5% at P10 to 35.0 ± 3.0% at P13 to 47.2 ± 2.1% at P28 ($P < 0.01$ in one-way ANOVA, Fig. 2A). The percentage of OFF RGCs also increased from 7.0 ± 4.3% at P10 to 10.8 ± 1.8% at P13 to 14.5 ± 1.7% at P28, but the change is not significant statistically due to the small number of OFF RGCs we were able to measure ($P > 0.05$ in one-way ANOVA, Fig. 2A). The percentages of all three classes of RGCs at P50 or P180 were not statistically different from those at P28 [(Liu *et al.*, 2007) and data not shown], suggesting that these developmental changes in laminar refinement were virtually complete by P28.

Overexpression of NT-3 Accelerates RGC Dendritic Laminar Refinement

Given that NT-3 has been shown to modify formation of neuronal processes, we examined whether overexpression of NT-3 affects the time course of refinement of ON-OFF RGCs into ON or OFF RGCs. We found fewer ON-OFF RGCs in NT-3 OE mice than in their littermate controls (Fig. 2E). At P13, 38.8 ± 3.9% of RGCs were ON-OFF in NT-3 OE mice, significantly lower than that in age-matched WT littermate controls (52.1 ± 3.6%, $P < 0.05$, Student's *t*-test, same below; Fig. 2E). The percentage of OFF RGCs were higher in NT-3 OE mice (14.1 ± 2.3% in NT-3 OE vs. 5.8 ± 1.3% in WT, $P < 0.05$), while ON RGCs were not significantly changed (47.1 ± 3.3% in NT-3 OE vs. 42.1 ± 3.1% in WT, $P = 0.29$, Fig. 2F). Two weeks after eye opening, at P28, NT-3 OE mice had 32.4 ± 1.0% ON-OFF RGCs, not significantly different from WT littermate mice (39.6 ± 6.7%, $P = 0.28$, Fig. 2E). These

data indicate that overexpression of NT-3 accelerates the rate of normal maturational laminar refinement before the time of eye opening.

We tested whether overexpression of NT-3 changed Thy-1-YFP expression. The above results might be skewed if the expression pattern of Thy-1-YFP was altered by overexpression of NT-3. We found similar numbers of Thy-1-YFP RGCs were labeled in NT-3 OE mice compared to their littermate WT controls at P13 (Fig. 2C). 32 ± 2 RGCs/retina in NT-3 OE mice (N = 7 retinas) and 33 ± 2 RGCs/retina in WT (N = 6 retinas) were found to express Thy-1-YFP transgene ($P = 0.87$). In addition, we examined an independently identified subclass of RGCs to test whether overexpression of NT-3 changed their representation in Thy-1-YFP RGCs. We double-labeled RGCs with SMI-32 (Liu *et al.*, 2007), which selectively marks 4 classes of RGC--M3, M7, M9 and M10 (Coombs *et al.*, 2006). Alternatively, using Sun *et al.*'s classification scheme, it appears that the SMI-32 positive ON RGCs fell into subgroups of RGC_{A1}, RGC_{C1}, and RGC_{C3} (Sun *et al.*, 2002). In WT retinas, 34.4 ± 7.1 % and 36.0 ± 5.6 % of RGCs were co-labeled with Thy-1-YFP and SMI-32 at P13 and P28, respectively (Fig. 2D). In NT-3 OE mice, 38.9 ± 2.1 % and 32.7 ± 5.0 % of Thy-1-YFP labeled neurons were also co-labeled with SMI-32 at P13 and P28, similar to that in WT mice (Fig. 2D, $P = 0.59$ at P13 and $P = 0.67$ at P28). These findings argue that NT-3 overexpression did not shift Thy1-YFP expression to other classes of RGCs, nor did it change the relative expression levels of Thy1-YFP.

RGC Dendritic Field Sizes Increase at Different Rates During Postnatal Development

Next, we quantified the development of dendritic arbor structure in WT and NT-3 OE mice. Fig. 3A–B shows dendritic field sizes at different postnatal ages. Z-stack images of YFP-expressing RGCs were projected as a 2-D image and dendritic coverage area was measured using NIH ImageJ (Diao *et al.*, 2004; Liu *et al.*, 2007). The distribution of dendritic field sizes shifted to the right from P10 (N = 58 RGCs) to P13 (N = 97 RGCs) to P28 (N = 121 RGCs), indicating that the dendritic fields subtended by the ensemble of RGCs increased from P10 to P28 ($P < 0.001$ in one-way ANOVA, Fig. 3A). The distribution of dendritic field areas subtended by all RGCs at P50 (N = 48 RGCs) was not significantly changed from P28 ($P > 0.05$ in one-way ANOVA, Fig. 3A).

Of particular interest, in terms of observing variable maturational patterns, we find that the dendritic arbors of ON, OFF and ON-OFF RGCs exhibit different growth rates (Fig. 3B and S-Table 1A). The mean dendritic coverage area subtended by ON RGC arbors kept expanding from P10 to P28; by contrast, the mean area covered by ON-OFF RGC arbors significantly increased only before eye opening (Fig. 3B and S-Table 1A). On the other hand, OFF RGC dendritic areas significantly increased only after eye opening (Fig. 3B and S-Table 1A). At P50, the dendritic field sizes of all three types of RGC are similar to those at P28 (Fig. 3B and S-Table 1A), suggesting that the dendritic field expansion was completed by P28.

Our findings are concordant with previous studies of laminar refinement and dendritic coverage in WT mouse retina (Badea and Nathans, 2004; Diao *et al.*, 2004; Landi *et al.*, 2007). For example, Landi *et al.* found that 65.8 ± 3.5% of RGCs were bi-stratified RGCs at P10 (Landi *et al.*, 2007), which is in agreement with our findings (65.9 ± 1.4%, Fig. 2A, B). We found that the mean dendritic field size subtended by ON-OFF RGCs at P13 was 22.7 ± 1.8 × 10^3 μm^2 (Fig. 3B), which fell in the range of 13.9–32.4 ×$10\mu^3$ μm^2 (dendritic field diameter: 133 – 203 μm) for bi-stratified subtype RGC_D (Diao *et al.*, 2004).

ON-OFF RGCs Exhibit Reduced Mean Branch Length and Increased Branch Number in NT-3 OE Mice

We examined whether overexpression of NT-3 modulates RGC dendritic field size. We found that the mean of the coverage area subtended by ON-OFF RGC arbors was significantly smaller in NT-3 OE mice than WT littermate controls at P13 ($P < 0.001$, Student's *t*-test; same below; Fig. 3C and S-Table 1B). Also, the relative distribution curves of arbor coverage showed that more ON-OFF RGCs had smaller dendritic fields than their WT controls (Fig. 3D). In contrast, the dendritic areas subtended by ON and OFF RGC arbors were not changed significantly by overexpression of NT-3 (ON: $P = 0.35$; OFF: $P = 0.81$; Fig. 3C and S-Table 1B).

Interestingly, the total dendritic lengths of ON-OFF RGC arbors were not different in NT-3 OE mice at P13 compared to WT mice ($3.47 \pm 0.23 \times 10^3$ μn NT-3 OE versus $3.36 \pm 0.17 \times 10^3$ μ WT; $P = 0.55$, Fig. 4A). Given the dendrites of ON-OFF RGCs in the NT-3 OE mice covered smaller areas but maintained the same overall dendritic length, we asked whether there were shorter but more numerous dendritic branches in these mice.

We found that ON-OFF RGCs in NT-3 OE mice had significantly more branches (163 ± 13, N = 32 RGCs) than that in the WT littermate controls (116 ± 9, N = 49 RGCs) at P13 ($P < 0.01$, Fig. 4B). The mean dendritic branch length of ON-OFF RGCs in NT-3 OE mice (24.6 ± 1.9 μas significantly shorter than in the WT littermate controls (29.8 ± 2.8 μm; $P < 0.001$, Fig. 4C).

We also examined the dendritic structure in ON RGCs (Fig. 4B-C). NT-3 overexpression increased branch number in ON RGCs ($P < 0.05$, Fig. 4B). The mean dendritic length of ON RGCs were not changed (NT-3 OE: 27.5 ± 2.2 μm, N = 32 RGCs; WT: 32.9 ± 2.6 μm, N = 39 RGCs; $P > 0.05$; Fig. 4C). These results are consistent with differential actions of NT-3 upon arbor formation in ON and ON-OFF RGCs. Our findings show NT-3 overexpression mainly caused the ON-OFF RGC dendritic arbors to have less expansive dendrites with more and shorter branches.

To address whether the measured decrease in branch length of ON-OFF RGCs might result from a loss of a population of ON-OFF RGCs that had longer dendrites, we analyzed a subset of ON-OFF RGCs that are selectively stained by SMI-32 (Fig. 5). Z-stack images of SMI-32 positive, YFP-expressing RGCs were projected to a single 2D-plane, and two representative images of ON-OFF RGCs from WT littermate control and NT-3 OE mice, respectively, are shown in Fig. 5A–B. We found that SMI-32 positive ON-OFF RGCs also showed decreased dendritic field sizes in NT-3 OE mice ($P < 0.001$). Moreover, NT-3 overexpression significantly increased the number of branches ($P < 0.01$) and decreased mean branch length ($P < 0.05$) in SMI-32 positive ON-OFF RGCs (Fig. 5C–D and S-Table 1C). In contrast, branch numbers and length in SMI-32 positive ON RGCs did not change significantly ($P > 0.05$; Fig. 5C–D and S-Table 1D). Taken together, these data support the notion that higher NT-3 levels during early neonatal development lead to smaller sized but more extensively branched dendrites in ON-OFF RGCs. Given that NT-3 OE increased branch numbers in the ensemble of ON RGCs but not the SMI-32 positive ON RGCs, we speculate that NT-3 affects a population of SMI-32 negative RGCs.

The Effects of NT-3-OE on ON-OFF RGC Dendritic Arbor Structures Persist Until at least P28

At P28, the mean coverage area of ON-OFF RGC arbors in NT-3OE mice remained significantly smaller compared to age-matched WT littermates but the mean total dendritic lengths were comparable (data not shown). Fig. 6A shows in the SMI-32 positive RGCs that the mean coverage area subtended by ON-OFF RGC arbors was significantly smaller in

NT-3 OE mice (17.0 ± 1.6 × 10^3 μm^2, N = 12 RGCs vs. 33.0 ± 1.8 × 10^3 μm^2, N = 15 RGCs in WT). The branch number of these ON-OFF RGCs was significantly higher in NT-3 OE mice (166 ± 12, N = 10 RGCs) compared to littermate WT controls (95 ± 8, N = 8 RGCs, $P < 0.001$). The mean dendritic length of these ON-OFF RGCs was significantly shorter in NT-3 OE mice (23.7 ± 2.0 μm) than littermate WT controls (59.6 ± 4.4 μm, $P < 0.001$ in Student's *t*-test, Fig. 6B, C).

Similarly as at P13, the mean coverage area subtended by SMI-32 positive ON RGC arbors were comparable in NT-3 OE mice at P28 (23.2 ± 2.4 × 10^3 μm^2, N = 15 RGCs) compared to WT controls (28.8 ± 2.5 × 10^3 μm^2, N = 20 RGCs; Fig. 6A). Branch numbers and length in these ON RGCs did not change significantly in NT-3 OE mice compared to littermate WT controls at P28 ($P > 0.05$, Student's *t*-test; Fig. 6B, C).

Discussion

In summary, this study shows that the progressive dendritic laminar refinement of RGCs from ON-OFF to ON or OFF cells in WT mice starts before eye opening, and continues for two weeks after eye opening. Overexpression of NT-3 accelerates this process before P13, suggesting that signaling via NT-3 could regulate the RGC dendritic laminar refinement before eye opening. This process is schematized in Fig. 7 (Upper left panel to lower right panel). By examining the fine structure of dendritic arbors, we further showed that ON, OFF, and ON-OFF RGCs acquire their dendritic structure and shape at different rates during neonatal development. Namely, the dendritic field size of ON RGCs grow both before and after eye opening, while ON-OFF RGCs expand mainly before eye opening and OFF RGCs after eye opening. Here we find marked contrasts between NT-3 and BDNF action on dendritic structures of different cell types in maturing neonatal retina (see model in Fig. 7). BDNF selectively promotes formation of new branches in ON but not ON-OFF RGCs (Liu *et al.*, 2007). NT-3 promotes formation of more, but shorter, branches selectively in ON-OFF RGCs. Taken together; our results suggest that NT-3 and BDNF play overlapping roles in laminar refinement and distinct roles in dendritic arborization during RGC postnatal development.

Different Subtypes of RGCs mature at Different Rates during Neonatal Development

RGCs are amongst the first retinal cells to differentiate before birth (Livesey and Cepko, 2001). After RGCs extend an axon into the optic nerve, a complex dendritic arbor soon takes shape with processes that diffusely ramify in the IPL during postnatal development (Sernagor *et al.*, 2001). Here we show that around 65% of RGCs were bi-laminated RGCs at P10, and the percentage decreased to around 35% at P28 (Fig. 1A). Our data imply that a majority of RGCs originate as ON-OFF RGCs and are "pruned" gradually into ON or OFF RGCs. However, it appears that not all RGCs are "born" as ON-OFF RGCs. Because ON RGCs can be identified soon after birth and a percentage of ON-OFF RGCs remains in adult, it seems that at least subclasses of ON and ON-OFF RGC are permanently specified by cell autonomous genetic programs around birth (Sernagor *et al.*, 2001). It is also possible that some ON-OFF cells may have developed from ON or OFF RGCs (Coombs *et al.*, 2007). Xu and Tian suggested that some cells actually start off as mono-stratified cells that span the sublamina *a/b* border and later some of these move to become OFF cells (Xu and Tian, 2007).

This study and previous ones validate that during postnatal development, RGC dendritic arbors continue to grow and refine through selective, cell specific regulated processes (Sernagor *et al.*, 2001). In kitten, the arbors of gamma RGCs are adult-like at birth, while the dendritic fields of alpha cells reach their adult dimensions three weeks after birth, around which time beta cell dendritic expansion begins (Dann *et al.*, 1988; Ault and Leventhal,

1994). We, and others, demonstrate that a subclass of bi-laminated ON-OFF RGCs are converted into mono-laminated ON or OFF RGCs, a process that starts before and continues after eye opening (Tian and Copenhagen, 2003; Landi *et al.*, 2007; Liu *et al.*, 2007; Xu and Tian, 2007; and the current study).

Laminar Refinement Before and After Eye Opening: Actions of BDNF and NT-3

Our studies indicate that laminar refinement, as assessed by the decreased percentage of ON-OFF RGCs, occurs across the age span from at least P10 until P28. This is true for animals raised in cyclic light/dark conditions. Both BDNF and NT-3 overexpressing mice have fewer ON-OFF RGCs at P13 than control mice [(Liu *et al.*, 2007) and Fig. 2E, F]. This finding strongly supports the idea that both of these neurotrophins accelerate the RGC laminar refinement before eye opening.

After eye opening RGC laminar refinement continues, but is retarded by visual deprivation (Tian and Copenhagen, 2003; Liu *et al.*, 2007). BDNF/TrkB signaling plays a role in mediating the light-dependent refinement as this process is halted in TrkB knockout mice (Liu *et al.*, 2007). Because NT-3 levels in retina are not changed by visual deprivation or across neonatal development (Fig. 1), we suggest that NT-3 does not play a role in laminar refinement after eye opening.

RGC Subtype-Specific Actions of BDNF and NT-3

Dendritic branch structures of ON-OFF RGCs exhibit shorter but more numerous branches and reduced dendritic coverage in mice with NT-3 overexpression (Figs. 3–5). In contrast, ON RGCs have more branches in BDNF overexpressing mice compared to age-matched controls (Liu *et al.*, 2007). Addition of branch number in ON RGCs is suppressed in dark reared animals and in TrkB hypomorphic mice (Liu *et al.*, 2007), suggesting that ON RGCs already formed before eye opening or a subset of ON-OFF RGCs that are converted to ON RGCs are selectively sensitive to BDNF/TrkB signaling.

Further study will be required to delineate which particular subtypes of ON and ON-OFF RGCs are sensitive to BDNF and NT-3. In our classification of neurons we grouped several subtypes of RGCs together. Thus the effects of NT-3 on the ON-OFF RGCs would include subtypes of RGC_{D1} and RGC_{D2} reported by Diao *et al.* (2004), or clusters 1, 2, and 3 of bistratified RGCs reported by Badea *et al.* (2004). The early postnatal expansion of dendritic arbors and actions of BDNF in ON RGCs would include one or more of the RGC_{A1}, RGC_{C1}, and RGC_{C3} subtypes classified by Sun *et al.* (2004) or clusters 1, 2, 8, and 9 of monostratified RGCs reported by Badea *et al.* (2004). We confirmed the actions of NT-3 and BDNF on subclasses of RGCs double-stained by SMI-32, which selectively marks 4 subclasses of RGC (Coombs *et al.*, 2006). Thus, one or more of these subtypes would be expected to preferentially sensitive to BDNF or NT-3; however, further sub classification at this time is not experimentally feasible due to lack of single cell-type specific RGC markers. We traced between 9 and 11 ON and ON-OFF RGCs in the retinas of control and NT-3 OE mice that were double-labeled by Thy-1-YFP and SMI-32 (Fig. 5). This limited number of cells may introduce a sampling bias because these GFP and SMI-32 positive ON or ON-OFF RGCs may not equally represent all 4 subclasses of RGC identified by SMI-32 (Coombs *et al.*, 2006). An ultimate goal will be to identify and characterize the actions of BDNF and NT-3 on single subclasses of RGCs.

How Does NT-3 Act on Neuronal Morphology in Retina?

Little is known of how diffusibleneurotrophins such as BDNF and NT-3 regulate the long-term functional and structural maturation of neurons during postnatal development (McAllister *et al.*, 1999; Poo, 2001). Trk (tropomyosin-related kinase) receptor tyrosine

kinase C (TrkC) is the primary high-affinity receptor for NT-3 (Huang and Reichardt, 2001). TrkC were found in most, if not all, RGCs (Rickman and Brecha, 1995; Hallbook *et al.*, 1996; Llamosas *et al.*, 1997; von Bartheld and Butowt, 2000), similar to NT-3 [but see the sparse expression of NT-3 in one mouse study (Bennett *et al.*, 1999)]. NT-3 may also bind to other low-affinity Trk receptors under different circumstances (Huang and Reichardt, 2001). For example, sensory ganglia in *trkC* mutant mice has less severe losses of neurons than those in *NT-3* null mutant mice, suggesting that NT-3 may signal through receptors other than TrkC *in vivo* (Tessarollo *et al.*, 1993; Tessarollo *et al.*, 1997). In the dorsal root ganglia, NT-3 is required for activation of TrkB during neurogenesis and TrkA during target tissue innervation (Farinas *et al.*, 1998; Coppola *et al.*, 2001). In addition, studies showed that NT-3 could activate the low-affinity receptor p75NTR, a member of the tumor necrosis factor (TNF) receptor family (Huang and Reichardt, 2001). P75NTR is found in the ganglion cell layer (Ugolini *et al.*, 1995; Llamosas *et al.*, 1997) and transmits signals important for neuron survival (Huang and Reichardt, 2001).

More examples suggest that activation of different Trk receptors could lead to different intracellular signaling cascades and different biological results (Huang and Reichardt, 2001; 2003). For example, TrkB and TrkCsignals activate Shc site-dependent and -independent pathways, respectively, to maintain target innervation (Postigo *et al.*, 2002). *In vitro* cell system studies suggest that BDNF and NT-3 signaling have different effectson the same target neuron (Song and Poo, 1999). In the developing neocortex, BDNF and NT-3 have opposingroles in regulating the growth of basal dendrites of pyramidalneurons (McAllister *et al.*, 1997). Despite significant progress in these areas, it remains to be established how activation of differentTrk receptors leads to similar and/or different biological consequences in the mammalian retina *in vivo*. Subtype-specific TrkC knockout mice in the retina are needed to investigate whether NT-3 activates through TrkC receptor to modulate RGC dendritic structure during postnatal development.

Supplementary Material

Refer to Web version on PubMed Central for supplementary material.

Acknowledgments

This work has been supported by a Knights Templar Research Grant (XL), Midwest Eye-Banks Research Grant (XL), That Man May See (DRC), Research to Prevent Blindness (DRC and MML), the Foundation Fighting Blindness (MML), and NIH-NEI grants R01EY001869 (DRC), R01EY012995 (MLR), R01EY018621 (JC), and R01EY019034 (XL).

References

Ault SJ, Leventhal AG. Postnatal development of different classes of cat retinal ganglion cells. J Comp Neurol. 1994; 339(1):106–116. [PubMed: 8106655]

Badea TC, Nathans J. Quantitative analysis of neuronal morphologies in the mouse retina visualized by using a genetically directed reporter. J Comp Neurol. 2004; 480(4):331–351. [PubMed: 15558785]

Bennett JL, Zeiler SR, Jones KR. Patterned expression of BDNF and NT-3 in the retina and anterior segment of the developing mammalian eye. Invest Ophthalmol Vis Sci. 1999; 40(12):2996–3005. [PubMed: 10549663]

Campbell MJ, Morrison JH. Monoclonal antibody to neurofilament protein (SMI-32) labels a subpopulation of pyramidal neurons in the human and monkey neocortex. J Comp Neurol. 1989; 282(2):191–205. [PubMed: 2496154]

Coombs J, van der List D, Wang GY, Chalupa LM. Morphological properties of mouse retinal ganglion cells. Neurosci. 2006; 140(1):123–136.

Coombs JL, Van Der List D, Chalupa LM. Morphological properties of mouse retinal ganglion cells during postnatal development. J Comp Neurol. 2007; 503(6):803–814. [PubMed: 17570502]

Coppola V, Kucera J, Palko ME, Martinez-De Velasco J, Lyons WE, Fritzsch B, Tessarollo L. Dissection of NT3 functions *in vivo* by gene replacement strategy. Development (Cambridge, England). 2001; 128(21):4315–4327.

Dann JF, Buhl EH, Peichl L. Postnatal dendritic maturation of alpha and beta ganglion cells in cat retina. J Neurosci. 1988; 8(5):1485–1499. [PubMed: 3367208]

Diao L, Sun W, Deng Q, He S. Development of the mouse retina: emerging morphological diversity of the ganglion cells. J Neurobiol. 2004; 61(2):236–249. [PubMed: 15389605]

Farinas I, Wilkinson GA, Backus C, Reichardt LF, Patapoutian A. Characterization of neurotrophin and Trk receptor functions in developing sensory ganglia: direct NT-3 activation of TrkB neurons *in vivo*. Neuron. 1998; 21(2):325–334. [PubMed: 9728914]

Feng G, Mellor RH, Bernstein M, Keller-Peck C, Nguyen QT, Wallace M, Nerbonne JM, Lichtman JW, Sanes JR. Imaging neuronal subsets in transgenic mice expressing multiple spectral variants of GFP. Neuron. 2000; 28(1):41–51. [PubMed: 11086982]

Gerrero MR, McEvilly RJ, Turner E, Lin CR, O'Connell S, Jenne KJ, Hobbs MV, Rosenfeld MG. Brn-3.0: a POU-domain protein expressed in the sensory, immune, and endocrine systems that functions on elements distinct from known octamer motifs. Proc Natl Acad Sci U S A. 1993; 90(22):10841–10845. [PubMed: 8248179]

Haeseleer F, Sokal I, Verlinde CL, Erdjument-Bromage H, Tempst P, Pronin AN, Benovic JL, Fariss RN, Palczewski K. Five members of a novel Ca(2+)-binding protein (CABP) subfamily with similarity to calmodulin. J Biol Chem. 2000; 275(2):1247–1260. [PubMed: 10625670]

Hallbook F, Backstrom A, Kullander K, Ebendal T, Carri NG. Expression of neurotrophins and trk receptors in the avian retina. J Comp Neurol. 1996; 364(4):664–676. [PubMed: 8821453]

Haverkamp S, Wassle H. Immunocytochemical analysis of the mouse retina. J Comp Neurol. 2000; 424(1):1–23. [PubMed: 10888735]

Huang EJ, Reichardt LF. Neurotrophins: roles in neuronal development and function. Annu Rev Neurosci. 2001; 24:677–736. [PubMed: 11520916]

Huang EJ, Reichardt LF. Trk receptors: roles in neuronal signal transduction. Annu Rev Biochem. 2003; 72:609–642. [PubMed: 12676795]

Johnson J, Sherry DM, Liu X, Fremeau RT Jr, Seal RP, Edwards RH, Copenhagen DR. Vesicular glutamate transporter 3 expression identifies glutamatergic amacrine cells in the rodent retina. J Comp Neurol. 2004; 477(4):386–398. [PubMed: 15329888]

Landi S, Cenni MC, Maffei L, Berardi N. Environmental enrichment effects on development of retinal ganglion cell dendritic stratification require retinal BDNF. PLoS ONE. 2007; 2(4):e346. [PubMed: 17406670]

Lavail MM, Nishikawa S, Duncan JL, Yang H, Matthes MT, Yasumura D, Vollrath D, Overbeek PA, Ash JD, Robinson ML. Sustained delivery of NT-3 from lens fiber cells in transgenic mice reveals specificity of neuroprotection in retinal degenerations. J Comp Neurol. 2008; 511(6):724–735. [PubMed: 18925574]

Liu X, Grishanin RN, Tolwani RJ, Renteria RC, Xu B, Reichardt LF, Copenhagen DR. Brain-derived neurotrophic factor and TrkB modulate visual experience-dependent refinement of neuronal pathways in retina. J Neurosci. 2007; 27(27):7256–7267. [PubMed: 17611278]

Livesey FJ, Cepko CL. Vertebrate neural cell-fate determination: lessons from the retina. Nat Rev Neurosci. 2001; 2(2):109–118. [PubMed: 11252990]

Llamosas MM, Cernuda-Cernuda R, Huerta JJ, Vega JA, Garcia-Fernandez JM. Neurotrophin receptors expression in the developing mouse retina: an immunohistochemical study. Anat Embryol. 1997; 195(4):337–344. [PubMed: 9108199]

McAllister AK, Katz LC, Lo DC. Opposing roles for endogenous BDNF and NT-3 in regulating cortical dendritic growth. Neuron. 1997; 18(5):767–778. [PubMed: 9182801]

McAllister AK, Katz LC, Lo DC. Neurotrophins and synaptic plasticity. Annu Rev Neurosci. 1999; 22:295–318. [PubMed: 10202541]

Nixon RA, Lewis SE, Dahl D, Marotta CA, Drager UC. Early posttranslational modifications of the three neurofilament subunits in mouse retinal ganglion cells: neuronal sites and time course in

relation to subunit polymerization and axonal transport. Brain Res Mol Brain Res. 1989; 5(2):93–108. [PubMed: 2469928]

Poo MM. Neurotrophins as synaptic modulators. Nature reviews. 2001; 2(1):24–32.

Postigo A, Calella AM, Fritzsch B, Knipper M, Katz D, Eilers A, Schimmang T, Lewin GR, Klein R, Minichiello L. Distinct requirements for TrkB and TrkC signaling in target innervation by sensory neurons. Genes Dev. 2002; 16(5):633–645. [PubMed: 11877382]

Rickman DW, Brecha NC. Expression of the proto-oncogene, trk, receptors in the developing rat retina. Vis Neurosci. 1995; 12(2):215–222. [PubMed: 7786843]

Robinson ML, Overbeek PA, Verran DJ, Grizzle WE, Stockard CR, Friesel R, Maciag T, Thompson JA. Extracellular FGF-1 acts as a lens differentiation factor in transgenic mice. Development (Cambridge, England). 1995; 121(2):505–514.

Segal RA, Pomeroy SL, Stiles CD. Axonal growth and fasciculation linked to differential expression of BDNF and NT3 receptors in developing cerebellar granule cells. J Neurosci. 1995; 15(7 Pt 1): 4970–4981. [PubMed: 7623126]

Seki M, Fukuchi T, Tanaka T, Nawa H, Takei N, Abe H. Quantitative analyses of mRNA and protein levels of neurotrophin-3 in the rat retina during postnatal development and aging. Jpn J Ophthalmol. 2004; 48(5):460–464. [PubMed: 15486768]

Seki M, Nawa H, Fukuchi T, Abe H, Takei N. BDNF is upregulated by postnatal development and visual experience: quantitative and immunohistochemical analyses of BDNF in the rat retina. Invest Ophthalmol Vis Sci. 2003; 44(7):3211–3218. [PubMed: 12824273]

Sernagor E, Eglen SJ, Wong RO. Development of retinal ganglion cell structure and function. Prog Retin Eye Res. 2001; 20(2):139–174. [PubMed: 11173250]

Song HJ, Poo MM. Signal transduction underlying growth cone guidance by diffusible factors. Curr Opin Neurobiol. 1999; 9(3):355–363. [PubMed: 10395576]

Sun W, Li N, He S. Large-scale morphological survey of mouse retinal ganglion cells. J Comp Neurol. 2002; 451(2):115–126. [PubMed: 12209831]

Tessarollo L, Tsoulfas P, Donovan MJ, Palko ME, Blair-Flynn J, Hempstead BL, Parada LF. Targeted deletion of all isoforms of the trkC gene suggests the use of alternate receptors by its ligand neurotrophin-3 in neuronal development and implicates trkC in normal cardiogenesis. Proc Natl Acad Sci U S A. 1997; 94(26):14776–14781. [PubMed: 9405689]

Tessarollo L, Tsoulfas P, Martin-Zanca D, Gilbert DJ, Jenkins NA, Copeland NG, Parada LF. trkC, a receptor for neurotrophin-3, is widely expressed in the developing nervous system and in non-neuronal tissues. Development (Cambridge, England). 1993; 118(2):463–475.

Tian N, Copenhagen DR. Visual stimulation is required for refinement of ON and OFF pathways in postnatal retina. Neuron. 2003; 39(1):85–96. [PubMed: 12848934]

Ugolini G, Cremisi F, Maffei L. TrkA, TrkB and p75 mRNA expression is developmentally regulated in the rat retina. Brain Research. 1995; 704(1):121–124. [PubMed: 8750972]

von Bartheld CS, Butowt R. Expression of neurotrophin-3 (NT-3) and anterograde axonal transport of endogenous NT-3 by retinal ganglion cells in chick embryos. J Neurosci. 2000; 20(2):736–748. [PubMed: 10632603]

Wassle H, Peichl L, Airaksinen MS, Meyer M. Calcium-binding proteins in the retina of a calbindin-null mutant mouse. Cell and tissue research. 1998; 292(2):211–218. [PubMed: 9560464]

Witkovsky P, Gabriel R, Krizaj D. Anatomical and neurochemical characterization of dopaminergic interplexiform processes in mouse and rat retinas. J Comp Neurol. 2008; 510(2):158–174. [PubMed: 18615559]

Xiang M, Gan L, Zhou L, Klein WH, Nathans J. Targeted deletion of the mouse POU domain gene Brn-3a causes selective loss of neurons in the brainstem and trigeminal ganglion, uncoordinated limb movement, and impaired suckling. Proc Natl Acad Sci U S A. 1996; 93(21):11950–11955. [PubMed: 8876243]

Xiang M, Zhou L, Macke JP, Yoshioka T, Hendry SH, Eddy RL, Shows TB, Nathans J. The Brn-3 family of POU-domain factors: primary structure, binding specificity, and expression in subsets of retinal ganglion cells and somatosensory neurons. J Neurosci. 1995; 15(7 Pt 1):4762–4785. [PubMed: 7623109]

Xu HP, Tian N. Retinal ganglion cell dendrites undergo a visual activity-dependent redistribution after eye opening. J Comp Neurol. 2007; 503(2):244–259. [PubMed: 17492624]

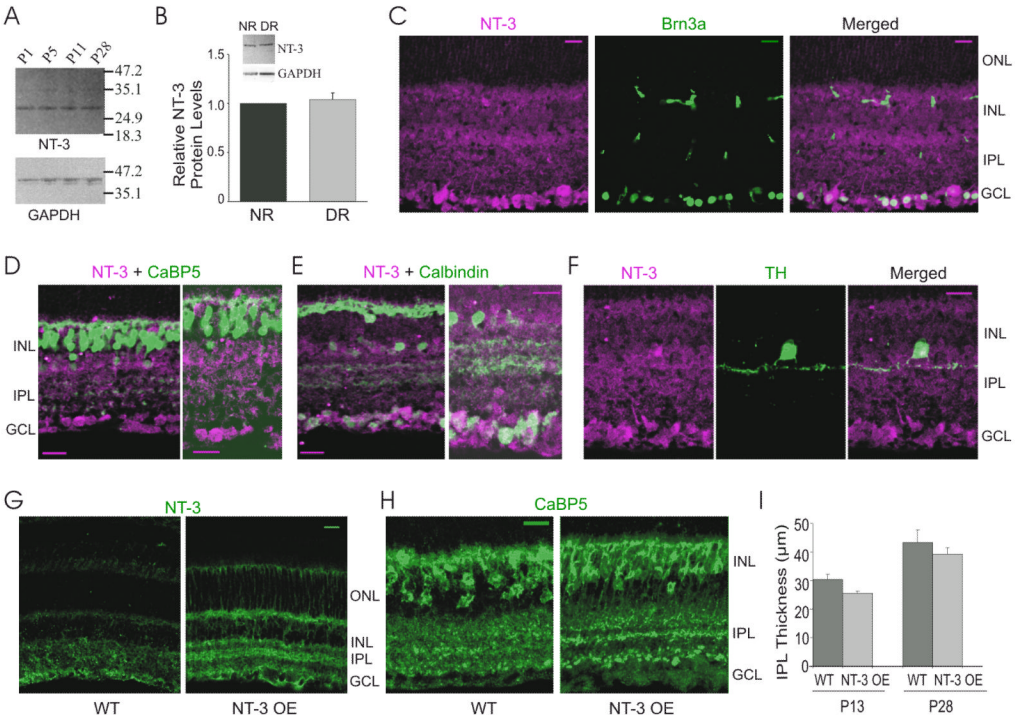

Figure 1.

NT-3 expression in retinas of wild type (WT) and NT-3 overexpressing (NT-3 OE) mice. (A) A representative Western blot analysis for NT-3 on retinal protein extracts isolated at different postnatal ages. GAPDH was used as an internal control of the loading. (B) Quantification of relative retinal NT-3 protein levels shows that dark rearing (DR) did not change NT-3 expression level compared to mice reared in 12hr dark/12hr light cycles (Normal Rearing, NR). A representative Western blot for NT-3 and GAPDH is inserted on the top. (C–F) Confocal fluorescence micrograph of WT mouse retina double immunostained with antibodies against NT-3 (magenta), and Brn-3a, CaBP5, calbindin and TH (green), respectively. (G–H) Confocal fluorescence micrographs of immunolabeling of NT-3 (G) and CaBP5 (H) in WT and NT-3 OE retinas. ONL, outer nuclear layer; INL, inner nuclear layer; IPL, inner plexiform layer; GCL, ganglion cell layer. Scale bar: 20 μm. (I) The IPL thickness increased from P13 to P28 in the WT retina and overexpression of NT-3 did not change the thickness of the IPL at P13 and P28. *:$P < 0.05$ in Student's *t*-test.

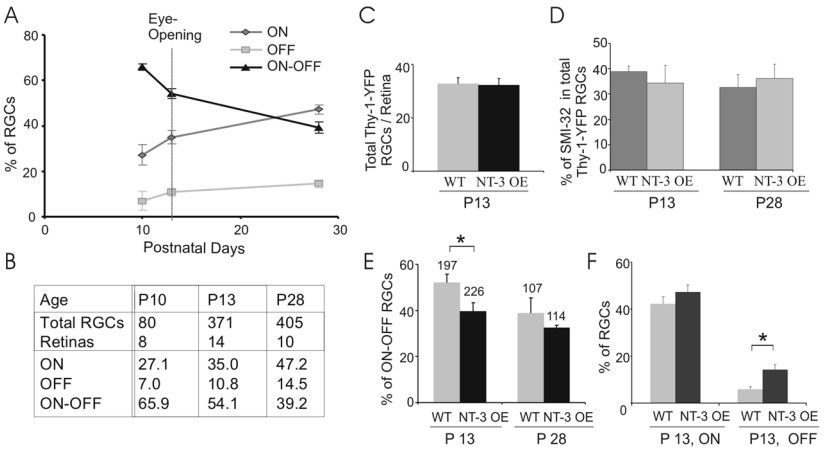

Age	P10	P13	P28
Total RGCs	80	371	405
Retinas	8	14	10
ON	27.1	35.0	47.2
OFF	7.0	10.8	14.5
ON-OFF	65.9	54.1	39.2

Figure 2.

Overexpression of NT-3 accelerates the conversion of ON-OFF RGCs to ON or OFF RGCs before eye opening. (A–B) Developmental profile of percentages of ON, OFF, and ON-OFF RGCs in WT retina from P10 to P28. Total numbers of RGCs and retinas counted at different ages are listed in (B). (C) The number of Thy-1-YFP labeled RGCs/retina was not changed in NT-3 OE mice at P13. (D) NT-3 OE did not change the percentage of RGCs double-labeled by SMI-32 and Thy-1-YFP at P13 and P28. (E) Comparisons of percentage of ON-OFF RGCs in NT-3 OE with their littermate WT control mice. The total numbers of RGCs counted at P13 and P28 are listed on the top. (F) Comparisons of percentages of ON and OFF RGCs in NT-3 OE and WT mice at P13. *: $P < 0.05$ in Student's *t*-test. Error bar represents the standard error of the mean (± S. E. M; same in Figs 3–6).

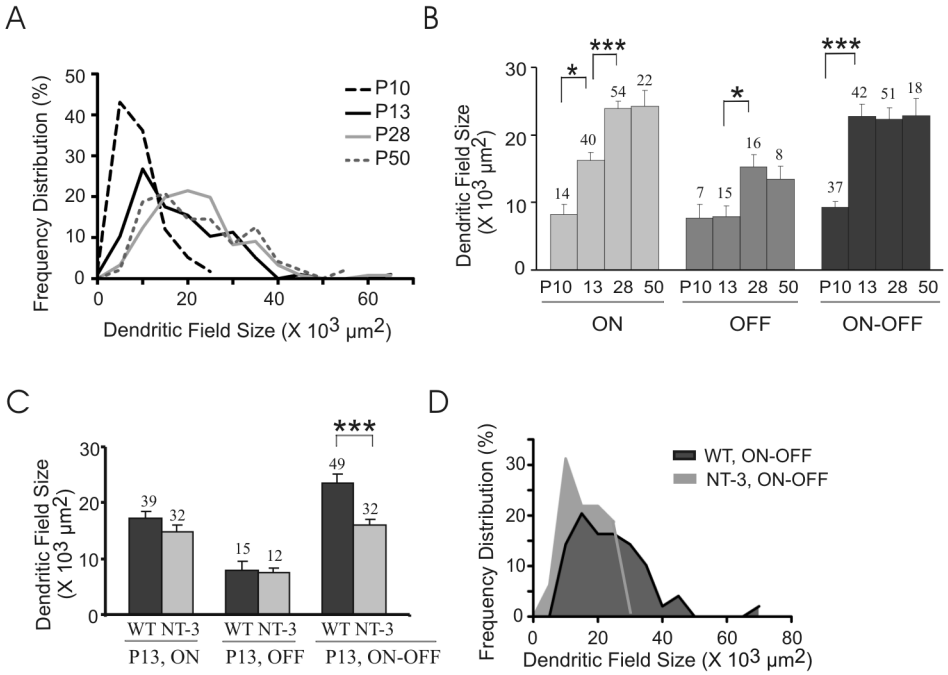

Figure 3.

Dendritic field sizes increase at different rates during postnatal development in WT mice (A–B) and overexpression of NT-3 significantly reduces the dendritic field size subtended by ON-OFF RGCs at P13 (C–D). (A) Histogram of RGC dendritic field sizes during postnatal development in WT mice. Bin width: 5000 μm^2. (B) Means of the dendritic field sizes of ON, OFF, and ON-OFF RGCs from P10 to P50. The total numbers of RGCs counted at each age for each subtype are listed on the top. *: $P < 0.05$; **: $P < 0.01$; ***: $P < 0.001$ in one-way ANOVA post Tukey's multiple comparison tests. (C) Overexpression of NT-3 significantly reduces the dendritic field size subtended by ON-OFF RGCs but not ON and OFF RGCs at P13. ***: $P < 0.001$ in Student's *t*-test. (D) Histogram of the dendritic field sizes in NT-3 OE and WT littermate control mice at P13. Bin width: 5000 μm^2.

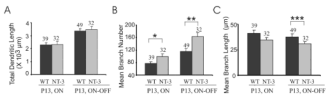

Figure 4.

NT-3 overexpression modulates the dendritic patterning of ON-OFF RGCs. (A) NT-3 OE did not change the total dendritic length of both ON and ON-OFF RGCs at P13. (B–C) NT-3 OE increases the branch number (B) and decreases mean branch length (C) of ON-OFF RGCs but not ON RGCs at P13. *: $P < 0.05$; **: $P < 0.01$; ***: $P < 0.001$ in Student's *t*-test (same in Figs 5–6).

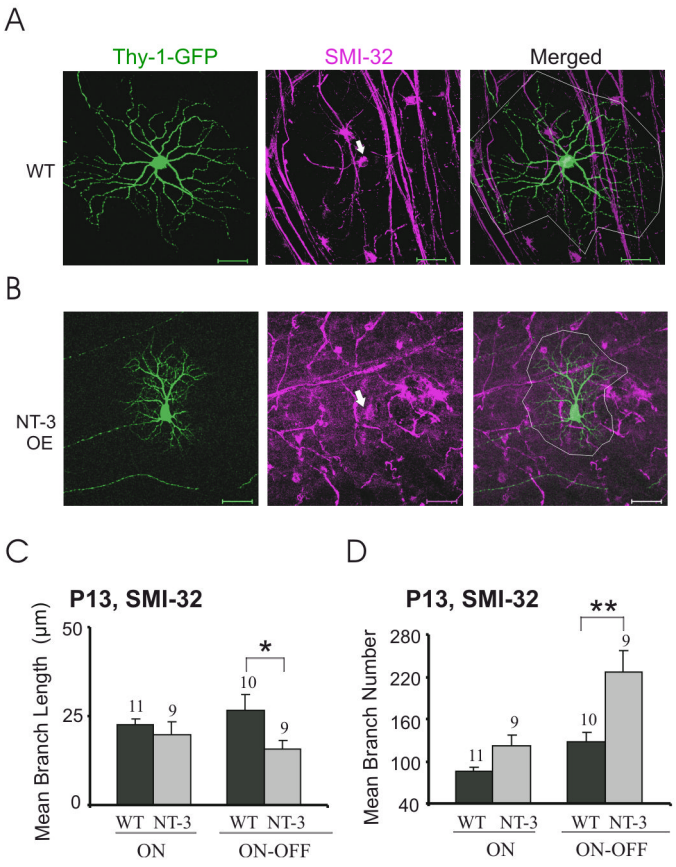

Figure 5.

Overexpression of NT-3 affects SMI-32 positive ON-OFF RGC dendritic structure at P13. (A–B) Z-stack confocal images of SMI-32 positive ON-OFF RGCs from littermate WT (A) and NT-3 OE (B) were projected to 2-D images and their dendritic field sizes were circled with white lines. Arrows point to the cell bodies of SMI-32 positive RGCs (magenta) doubled labeled with Thy-1-YFP (green). Scale bar: 50 μm. (C–D) Overexpression of NT-3 (labeled as NT-3) increased the branch number but decreased the branch length in SMI-32 positive ON-OFF RGCs, and did not affect the dendritic pattern of SMI-32 positive ON RGCs.

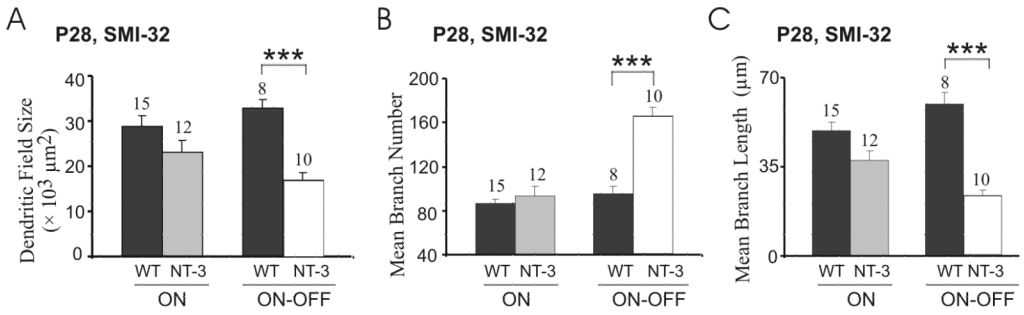

Figure 6.

The effects of NT-3 overexpression on ON-OFF RGC dendritic structure persist at P28. (A) Whereas NT-3 OE did not change the dendritic field size of ON RGCs double-labeled with SMI-32, it decreased the dendritic field size of ON-OFF RGCs double-labeled with SMI-32. (B–C) The branch number of SMI-32 positive ON-OFF RGCs increased (B) and their mean dendritic length decreased (C) in NT-3 OE mice at P28.

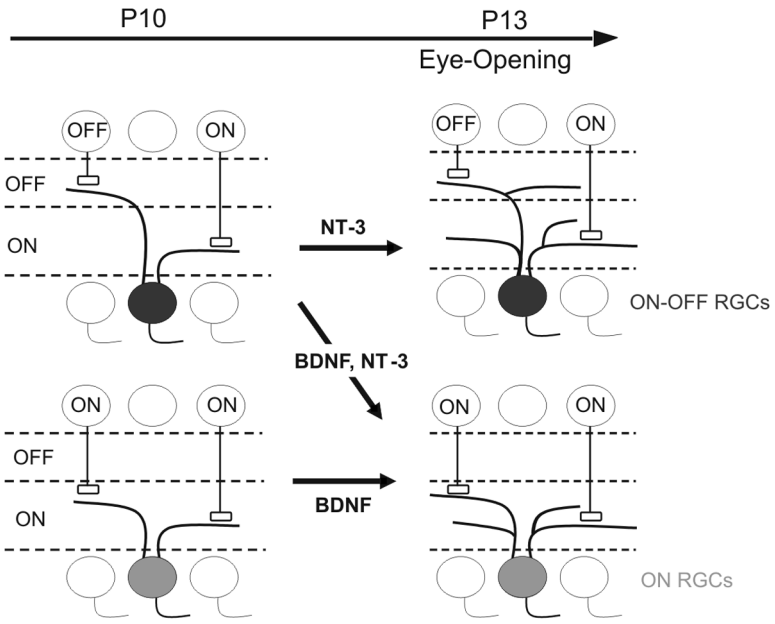

Figure 7.

Simplified model illustrating the refinement of RGC dendritic structure before eye opening [see details in this paper and (Liu *et al.*, 2007)]. The conversion of initially diffuse dendritic arbors of ON-OFF RGCs into mono-laminated ON RGCs begins prior to eye opening and continues after eye opening. Overexpression of BDNF and NT-3 accelerates this process by the time of eye opening (P13). While NT-3 mainly increases the branch number and decreases branch length of ON-OFF RGCs, BDNF increases the branching number of ON RGCs at P13.

Table 1

List of Primary Antibodies

Antigen	Host	Source	Catalog #	Poly/Mono	Dilution
Brn-3a	Mouse	Chemicon International, Temecula, CA	MAB1585	M	1:25–1:50
Calbindin	Mouse	Sigma-Aldrich, St. Louis, MO	C9848	M	1:500
GFP, Alexa Fluor® 488 conjugate	Rabbit	Invitrogen, Carlsbad, CA	A21311	P	1:1,000
NT-3	goat	R&D Systems, Minneapolis, MN	AF-267-NA	P	1: 200 (immuno); 1:500 (Western)
Tyrosine Hydroxylase (TH)	Mouse	Chemicon International, Temecula, CA	MAB318	M	1:100
Calcium Binding protein5 (CaBP5)	Rabbit	Dr. Krzysztof Palczewski, Case Western Reserve University, Cleveland, Ohio	Gift (See Ref.)	P	1:500
SMI-32	Mouse	Covance, Princeton, NJ	SMI-32R	M	1:1000